

Gas permeability versus texture relationship of sediment samples from a research well in the Beaufort-Mackenzie Basin, Northwest Territories

T.J. Katsube and S. Connell-Madore

2008

Geological Survey of Canada
Current Research 2008-4



Natural Resources Canada
Ressources naturelles Canada

Canada

©Her Majesty the Queen in Right of Canada 2008

ISSN 1701-4387

Catalogue No. M44-2008/4E-PDF

ISBN 978-0-662-47695-5

A copy of this publication is also available for reference in depository libraries across Canada through access to the Depository Services Program's Web site at <http://dsp-psd.pwgsc.gc.ca>

A free digital download of this publication is available from GeoPub:
http://geopub.nrcan.gc.ca/index_e.php

Toll-free (Canada and U.S.A.): 1-888-252-4301

Critical reviewers

Barbara Medioli

Marc Hinton

Authors

T.J. Katsube

(jkatsube@nrcan.gc.ca)

S. Connell-Madore

(sconnell@nrcan.gc.ca)

Geological Survey of Canada

601 Booth Street

Ottawa, Ontario K1A 0E8

Publication approved by GSC-Northern Canada

Correction date:

**All requests for permission to reproduce this work, in whole or in part, for purposes of commercial use, resale, or redistribution shall be addressed to: Earth Sciences Sector Copyright Information Officer, Room 644B, 615 Booth Street, Ottawa, Ontario K1A 0E9.
E-mail: ESSCopyright@NRCan.gc.ca**

Gas permeability versus texture relationship of sediment samples from a research well in the Beaufort-Mackenzie Basin, Northwest Territories

T.J. Katsube and S. Connell-Madore

Katsube, T.J. and Connell-Madore, S., 2008: Gas permeability versus texture relationship of sediment samples from a research well in the Beaufort-Mackenzie Basin, Northwest Territories; Geological Survey of Canada, Current Research 2008-4, 10 p.

Abstract: Relationships between gas permeability (k_G) and sediment texture have been examined for 28 sediment samples with different grain-size distributions. The purpose was to examine the required texture characteristics for an effective seal. These samples are from 908.05 m to 1090.89 m depths in a well in northern Canada. Increased clay content is expected to decrease fluid permeability and increase seal capacity.

Results show that grain sizes larger than fine sand ($>63 \mu\text{m}$) form the framework grains of these sediments. In this case, the mud fraction ($<63 \mu\text{m}$), consisting of clay and silt, forms the intergranular pore-filling material of these framework grains. When the smaller framework grains fill intergranular pore spaces of the larger framework grains, they reduce the pore space for mud to fill and contribute to reduced permeability and increased seal capacity. Although the main purpose of a seal is restricting liquid leakage, these gas permeability tests have produced useful information.

Résumé : Les rapports entre la perméabilité aux gaz (k_G) et la texture des sédiments ont été étudiés à partir de 28 échantillons de sédiments présentant des répartitions de la taille des grains différentes, afin d'identifier les propriétés texturales garantes d'une étanchéité efficace. Les échantillons analysés ont été prélevés à des profondeurs allant de 908,05 à 1090,89 m, dans un puits du Nord du Canada. Les résultats attendus sont à l'effet que la perméabilité aux fluides diminue et que l'étanchéité augmente à mesure que la teneur en argile s'accroît.

Les résultats obtenus montrent que les grains d'une taille supérieure à celle d'un sable fin ($> 63 \mu\text{m}$) constituent la charpente de ces sédiments. La fraction de la boue ($< 63 \mu\text{m}$), composée d'argile et de silt, remplit alors les pores entre les grains de charpente. Lorsque des grains de charpente plus petits remplissent l'espace interstitiel entre des grains de charpente plus gros, ils réduisent l'espace poral que la boue pourrait remplir et contribuent ainsi à réduire la perméabilité et à accroître l'étanchéité. Bien que l'étanchéité soit une caractéristique qui consiste principalement à limiter les fuites de liquides, ces essais de perméabilité aux gaz ont permis de générer de l'information utile.

INTRODUCTION

The relationship between gas permeability (k_G) and sediment texture has been examined for twenty-eight sediment samples with different grain-size distributions. The purpose was to examine the required texture characteristics for these unconsolidated sediments to perform as an effective seal. These samples are from a depth range of 908.05 m to 1090.89 m in the Mallik 2002 gas hydrate production research well (Mallik 5L-38 research well) in the Beaufort-Mackenzie Basin, Northwest Territories, northern Canada. This well was drilled as part of the JAPEX/JNOC/GSC gas hydrate project of 2003 (Dallimore et al., 2005)

It is well known that an increased clay content has a decreasing effect on fluid permeability and increases the seal capacity of a sediment. These 28 sediment samples consist of fine- to coarse-grained material, ranging from clay-sized grains to coarse sand (Connell-Madore and Katsube, 2007). In sedimentary formations, the coarse-grained material forms the framework grains (Katsube et al., 1998) with intergranular pores that contribute to fluid migration and increased permeability. On the other hand, the fine-grained material fills these intergranular pore spaces and contributes to blocking of the fluid migration and reduced permeability.

Table 1. Sample descriptions and gas permeability (k_G) values for the Mallik 5L-38 research well, listed in order of increasing depth (Katsube et al., 2005; Connell-Madore and Katsube, 2007).

Sample number	Depth (m)	Lithology	Gas permeability, k_G (mD)
P2EJA-11	908.05	Fine sand	1419
P2EJA-26	910.61	Fine sand	4062
P2EJA-16	916.19	Fine sand	5209
P2EJA-17	918.95	Fine sand	4963
P2EJA-21	920.81	Fine sand	3687
P2EJA-27	925.09	Fine sand	1813
P2EJA-7	927.35	Fine sand	4910
P2EJA-25	933.58	Clay	2.85
P2EJA-4	937.47	Clay	1.55
P2EJA-13	939.88	Clay	0.43
P2EJA-19	953.47	Silty sand	236
P2EJA-2	955.69	Medium sand	6957
P2EJA-20	972.05	Clay	2.15
P2EJA-14	973.08	Sand with organic material	1590
P2EJA-22	975.67	Silty sand	2464
P2EJA-5	980.65	Fine sand	3546
P2EJA-10	982.59	Clay	0.37
P2EJA-28	987.53	Fine sand	1091
P2EJA-1	989.73	Fine sand	3257
P2EJA-8	1004.93	Clay	0.12
P2EJA-24	1022.42	Fine sand	1904
P2EJA-15	1028.78	Clay	0.61
P2EJA-9	1042.12	Clay	0.54
P2EJA-18	1063.47	Organic shale, clayey coal	0.43
P2EJA-12	1072.75	Silty sand	194
P2EJA-6	1076.63	Fine sand	2658
P2EJA-3	1083.45	Clay	0.32
P2EJA-23	1089.89	Fine sand	1430

A considerable amount of work has been carried out in the past on the relationship between permeability and grain sizes (e.g. Masch and Denny, 1966; Domenico and Schwartz, 1990); however, these generally do not consider seal quality and have shown little consideration related to the effect of clay. The effect of clay is one of the main subjects in a recent paper related to seal quality (e.g. Yang and Aplin, 2007); however, limited consideration was given to the effect of the framework grain sizes in that paper. For these reasons, this paper focuses on the framework grain-size combinations and grain sizes of pore-filling material. A recent study (Connell-Madore and Katsube, 2007), using the same samples as in this paper, provides an indication of the possible significance that the framework grain-size combinations has on permeability; however, the effect of pore-filling material was not a focus in that study. In this paper, following the description of the methods of data acquisition, some sediment-texture models related to seal capacity are introduced and their possible effect on the pore-filling material versus seal quality relationship are discussed.

METHOD OF INVESTIGATION AND RESULTS

Two specimens were taken from each of the 28 samples (Table 1) and prepared for the grain-size analysis and gas permeability (k_G) tests (Connell-Madore and Katsube, 2007). These specimens were sent to AGAT Laboratories (Calgary, Alberta) for the analyses and tests. The k_G data used in this study have been previously published (Katsube et al., 2005) and the grain-size distribution data used in this study have recently been published (Connell-Madore and Katsube, 2007). Grain-size distribution data for samples from the same Mallik 5L-38 research well, including the 28 samples used in this study, are also available in a published database (Medioli et al., 2005), but in less detail. The grain-size distribution data in the recent publication (Connell-Madore and Katsube, 2007) have 92 data points per sample for the grain-size range of 0.4 μm to 2000 μm . The grain-size data in the database (Medioli et al., 2005) have 18 data points per sample, but for a larger number of samples (213 samples) and for a slightly wider depth range (885.88–1150.49 m). Most details of the analytical techniques used to produce these data are described in the references listed within those publications (Katsube et al., 2005; Medioli et al., 2005). For example, the k_G has been determined by routine petrophysical measuring techniques in accordance to the American Petroleum Institute's recommended practices for core-analysis procedure (American Petroleum Institute, 1960). These specimens were dried at a temperature of 80°C and measured at a temperature of 20–21°C. The k_G and grain-size distribution data used in this study are listed in Table 1 and Table 2, respectively.

Table 2. Volume percentages of the different grain-size fractions for the 28 samples from the Mallik 5L-38 research well (Connell-Madore and Katsube, 2007).

Sample number	Differential volume (%)							Total
	Clay <3.9 μm	Silt 3.9–63 μm	Very fine sand 63–125 μm	Fine sand 125–250 μm	Medium sand 250–500 μm	Coarse sand 500–1000 μm	Very coarse sand 1000–2000 μm	
P2EJA-1	4.61	14.42	12.04	27.27	41.96	0.32	0.00	100.00
P2EJA-2	1.37	3.94	6.39	8.86	42.32	34.05	3.10	99.97
P2EJA-3	20.70	20.99	9.97	5.87	0.77	0.00	0.00	100.01
P2EJA-4	18.24	54.97	14.35	16.37	4.21	0.00	0.00	100.04
P2EJA-5	4.66	13.31	9.02	26.53	47.98	0.00	0.00	99.98
P2EJA-6	4.81	15.59	11.32	36.18	32.86	0.01	0.00	100.01
P2EJA-7	3.68	11.59	7.95	18.80	54.65	3.45	0.00	100.01
P2EJA-8	19.58	63.49	12.80	15.87	0.06	0.00	0.00	100.01
P2EJA-9	30.85	30.85	0.41	0.00	0.00	0.00	0.00	100.01
P2EJA-10	26.79	77.05	7.83	1.34	0.05	0.00	0.00	100.02
P2EJA-11	7.69	23.88	14.03	37.52	18.59	0.00	0.00	99.99
P2EJA-12	15.51	42.55	29.54	16.79	0.00	0.00	0.00	100.00
P2EJA-13	21.41	83.54	4.07	0.56	0.00	0.00	0.00	99.99
P2EJA-14	7.03	21.19	6.32	15.64	41.26	8.28	2.94	99.98
P2EJA-15	25.30	25.30	3.13	0.38	0.00	0.00	0.00	100.01
P2EJA-16	1.46	3.76	15.85	57.94	16.53	2.65	0.90	100.03
P2EJA-17	2.09	5.44	11.96	69.03	11.53	0.00	0.00	99.98
P2EJA-18	25.81	70.70	12.99	13.81	0.06	0.00	0.00	100.02
P2EJA-19	6.21	22.73	34.10	35.03	0.15	0.00	0.00	99.99
P2EJA-20	23.95	65.78	13.55	1.63	0.00	0.00	0.00	100.02
P2EJA-21	2.62	6.94	17.39	61.49	10.80	0.00	0.00	99.95
P2EJA-22	5.93	16.39	10.67	26.78	41.20	1.27	0.00	100.00
P2EJA-23	6.02	20.18	17.33	27.67	28.61	0.09	0.00	100.01
P2EJA-24	4.56	15.49	15.71	29.84	33.52	0.01	0.00	100.00
P2EJA-25	9.88	37.10	24.80	28.70	0.15	0.00	0.00	100.03
P2EJA-26	2.78	8.36	7.79	20.75	46.35	12.41	2.17	100.00
P2EJA-27	4.14	12.32	21.36	52.64	8.76	0.00	0.00	100.04
P2EJA-28	13.53	38.20	13.94	36.19	3.65	0.00	0.00	100.04

DATA ANALYSIS

The grain-size distributions for these 28 samples from the recent publication (Connell-Madore and Katsube, 2007) are shown in Figure 1. Some grain-size distribution modes displayed in Figures 1a and 1b can actually consist of more than one or two modes. For example, many of the grain-size modes in Figure 1a suggest the possibility of such cases. In this study, the Wentworth grain-size classification system (Folk, 1968) is used for classification of the different grain sizes. Accordingly, the grain-size ranges for the 28 samples in this study are classified into clay (<3.9 μm), silt (3.9–63 μm), very fine sand (63–125 μm), fine sand (125–250 μm), medium sand (250–500 μm), coarse sand (500–1000 μm), and very coarse sand (1000–2000 μm) and listed in Tables 2 and 3. This classification system also uses mud (<63 μm) as one of its classes, which is a combination of clay and silt.

The relationships between the sand volume fractions and the gas permeability (k_G) are shown in Figure 2a, and the relationships between the clay and silt volume fractions against the k_G are shown in Figure 2b. The sand versus k_G relationships in Figure 2a are rather complex, but a general increase of medium sand (MS) and fine sand (FS) with increased k_G can be seen. The very fine sand (VFS) fraction initially

appears to increase with increased k_G , but then is followed by a decrease. On the basis of these results, although rather complex, the sand fractions can generally be considered as framework grains that contribute to increased intergranular pore space and fluid migration. In Figure 2b, both grain-size volume fractions (clay and silt) decrease with increased k_G . This suggests that these two fractions, or the mud fraction, can be considered as pore-filling material that block fluid migration.

In Figures 3 and 4 the differential volume values for the Wentworth grain sizes of the sand fractions are displayed. All samples contain a certain amount of clay and silt, or mud (<63 μm), but the samples with a mud content above 60% are not included in these diagrams. In addition, only the sections for the grain-sizes above 63 μm are displayed in these diagrams. This is because the main purpose of these diagrams is to display the framework grain combinations that would contribute to fluid migration. For example, samples P2EJA-4, P2EJA-18, and P2EJA-20, which have mud contents above 60%, contain some sand grain size (very fine sand and fine sand) fractions of 10–20% (Table 3) with other sand fractions below 5%. In such cases, it is questionable whether such low sand fractions could act as framework grains and contribute to fluid migration, so that these samples have not been included in these diagrams.

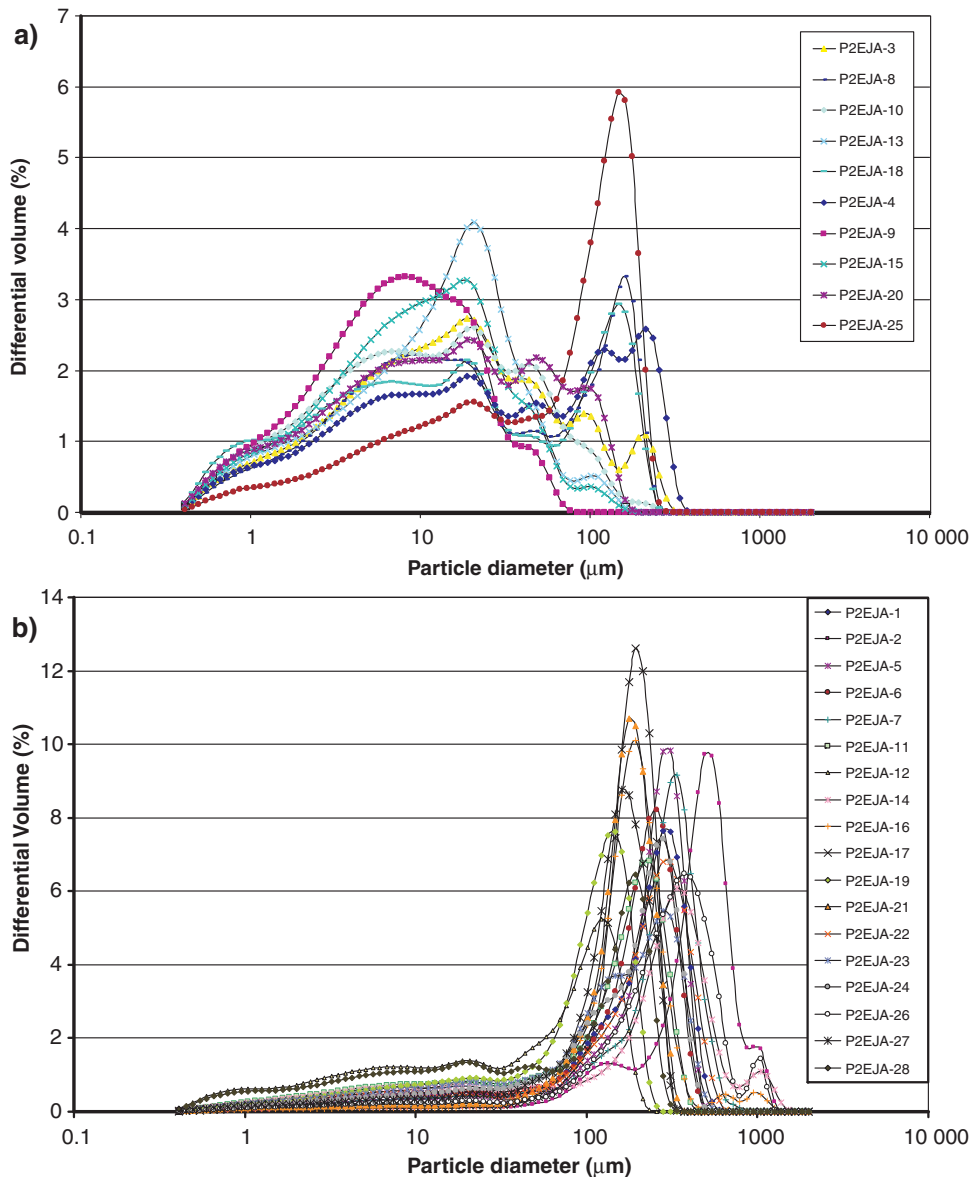


Figure 1. Grain-size distributions for **a)** ten clay-rich samples and **b)** eighteen sandy samples, both groups from the Mallik 5L-38 research well, Northwest Territories (Connell-Madore and Katsube, 2007).

When the differential volume values of the sand fractions in Figures 3 and 4 are reasonably large, that is at least 1.5 times the values of the rest, they are considered as differential volume maximums (with arrows displayed above them in the figures). Some samples show only one differential volume maximum, but others show two maximums. Figures 3 and 4 display the sample groups with one and two differential volume maximums, respectively. In Table 3 the 28 samples are grouped into those that show one (groups 1A, 1B, 1C) and two (groups 2A, 2B) differential volume maximums and a mud content (<63 μm) of above 60% (Group Ca). In that table, a column for mud (3.9–63 μm) has been added.

Gas permeability (k_G) as functions of mud content are shown in Figure 5. The data points are grouped into samples with one differential volume maximum (Group 1-DVM),

two differential volume maximums (Group 2-DVM), and a mud content above 60% (Group ‘Mud’). As seen in this figure, the k_G values decrease with increased mud content for the two sand sample groups (groups 1-DVM and 2-DVM) which have mud content values below 60%, as would be expected. Figure 5 shows that the sand sample k_G –mud-content relationships slightly differ between that for the group of samples with the one differential volume maximum and that with two differential volume maximums. The k_G –mud-content relationship for the latter is slightly steeper than the one for the samples with only one differential volume maximum. All samples in the ‘mud’ group have k_G values below 3 mD and more than 70% of those have k_G values below 1 mD. Those in the latter subgroup, surprisingly, show a slight general k_G increase with the increased mud content.

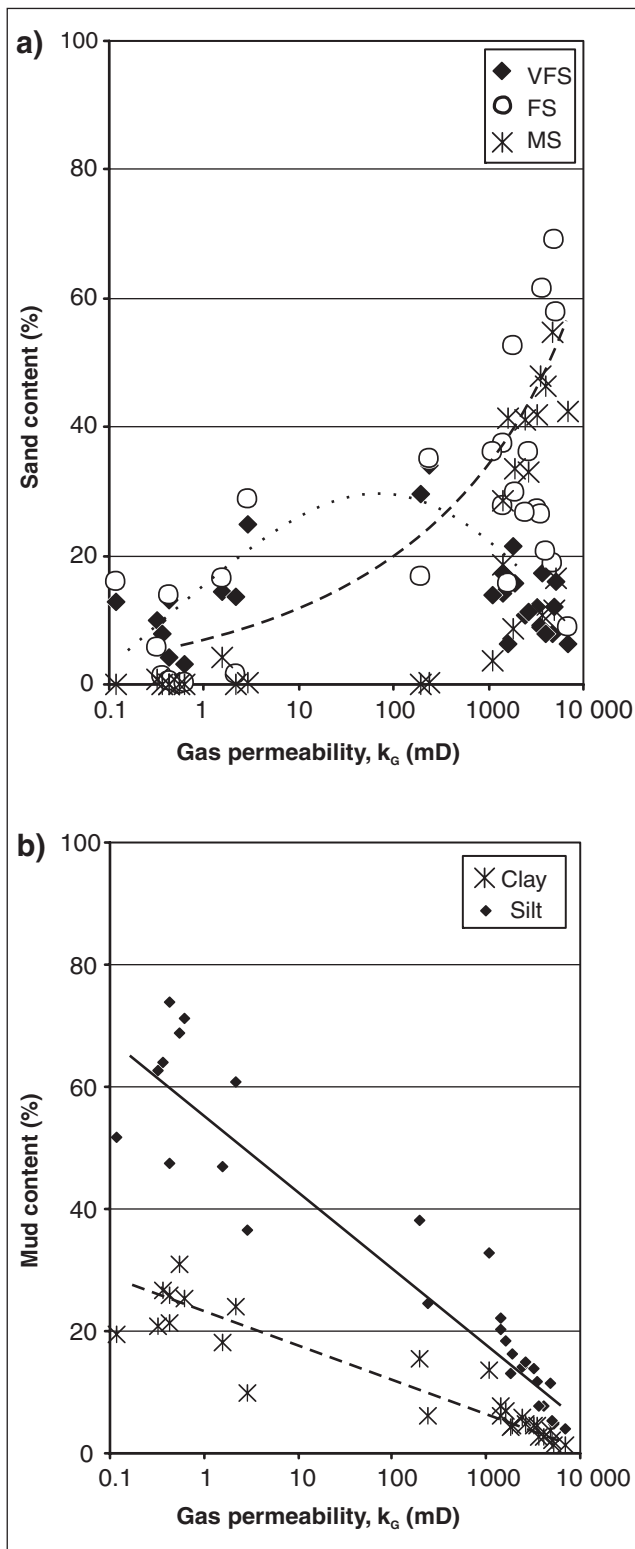


Figure 2. The relationships **a)** between sand volume fractions and gas permeability (k_g), and **b)** between mud volume fractions and k_g . VFS = very fine sand, FS = fine sand, MS = medium sand. Mud represents the volume fractions of silt and clay in this diagram.

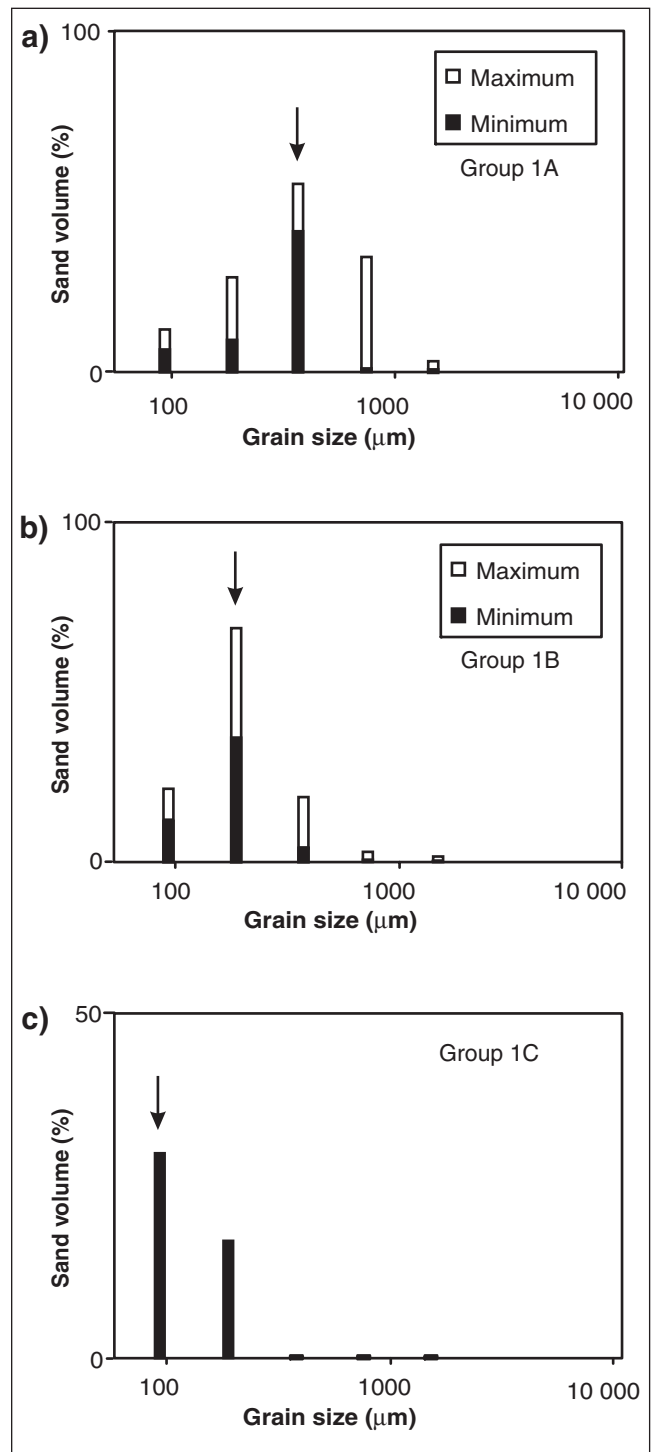


Figure 3. Differential volume values of the sand fractions for sample groups 1A, 1B, and 1C with one differential volume maximum (DVM) (arrow above). Only the sections above the mud grain-sizes ($>63 \mu\text{m}$) are displayed for each sample group. The sand fractions consist of very fine sand (63–125 μm), fine sand (125–250 μm), medium sand (250–500 μm), coarse sand (500–1000 μm), and very coarse sand (1000–2000 μm) as listed in Table 3.

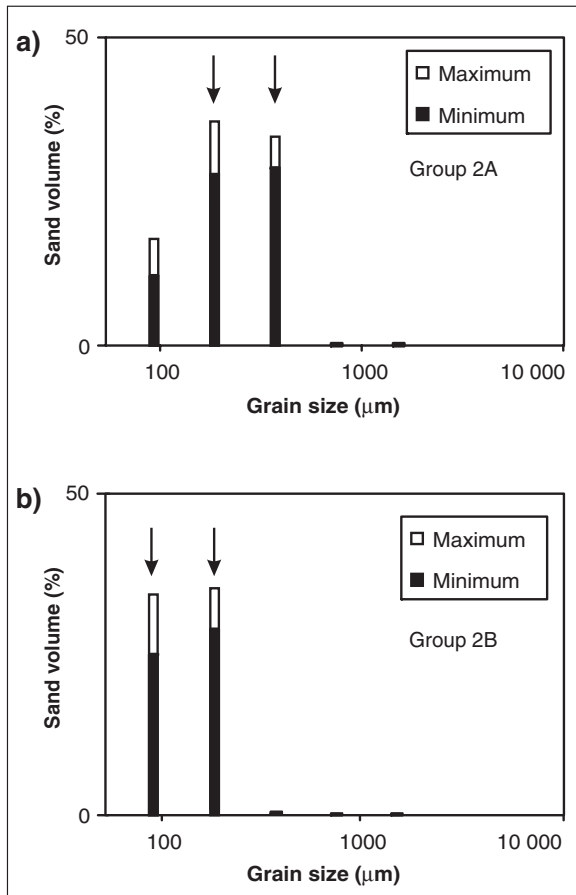


Figure 4. Differential volume values of the sand fractions for sample groups 2A and 2B with two differential volume maximums (arrows above). Only the sections above the mud grain sizes (>63 μm) are displayed for each sample group. The sand fractions consist of very fine sand (63–125 μm), fine sand (125–250 μm), medium sand (250–500 μm), coarse sand (500–1000 μm), and very coarse sand (1000–2000 μm) as listed in Table 3.

Figure 5. Gas permeability (k_g) as a function of mud content (<63 μm) for samples with one differential volume maximum (1-DVM), two differential volume maximums (2-DVM), and those (Mud) with a mud content above 60%.

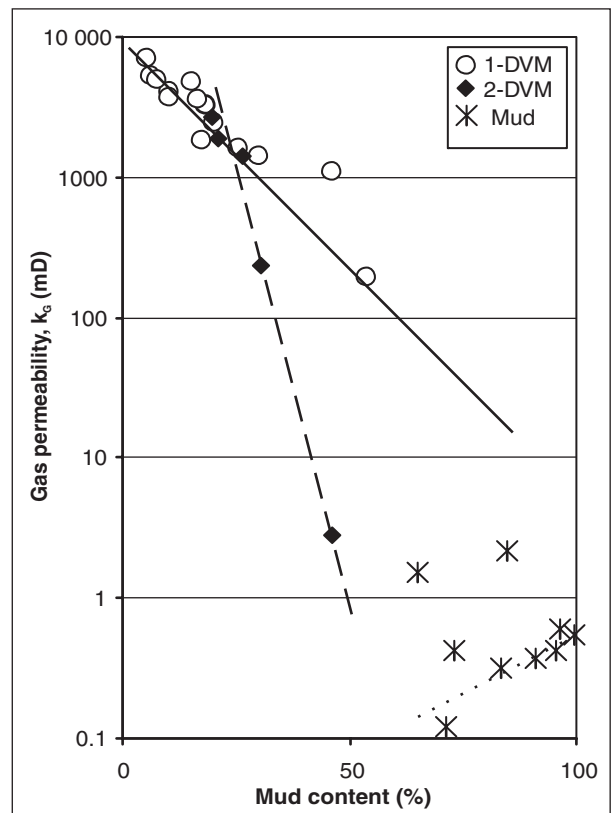


Table 3. Volume percentages of the different grain-size fractions for the 28 samples listed by groups (1A, 1B, 1C, 2A, and 2B) defined in Figures 3 and 4, and for samples with mud (clay+silt) content above 60% (Group Ca). Columns with bold numbers represent the differential volume maximums of the sample group.

Group/sample number		Differential volume (%)								Total
		Clay <3.9 μm	Silt 3.9–63 μm	Mud <63 μm	Very fine sand 63–125 μm	Fine sand 125–250 μm	Medium sand 250–500 μm	Coarse sand 500–1000 μm	Very coarse sand 1000–2000 μm	
1A	P2EJA-1	4.61	13.80	18.41	12.04	27.27	41.96	0.32	0.00	100.00
	P2EJA-2	1.37	3.88	5.25	6.39	8.86	42.32	34.05	3.10	99.99
	P2EJA-5	4.66	11.79	16.45	9.02	26.53	47.98	0.00	0.00	99.98
	P2EJA-7	3.68	11.48	15.16	7.95	18.80	54.65	3.45	0.00	100.01
	P2EJA-14	7.03	18.51	25.54	6.32	15.64	41.26	8.28	2.94	99.98
	P2EJA-22	5.93	14.15	20.08	10.67	26.78	41.20	1.27	0.00	100.00
	P2EJA-26	2.78	7.75	10.53	7.79	20.75	46.35	12.41	2.17	100.00
1B	P2EJA-11	7.69	22.16	29.85	14.03	37.52	18.59	0.00	0.00	99.99
	P2EJA-16	1.46	4.70	6.16	15.85	57.94	16.56	2.65	0.90	100.06
	P2EJA-17	2.09	5.37	7.46	11.96	69.03	11.53	0.00	0.00	99.98
	P2EJA-21	2.62	7.65	10.27	17.39	61.49	10.80	0.00	0.00	99.95
	P2EJA-27	4.14	13.14	17.28	21.36	52.64	8.76	0.00	0.00	100.04
	P2EJA-28	13.53	32.74	46.27	13.94	36.19	3.65	0.00	0.00	100.05
1C	P2EJA-12	15.51	38.16	53.67	29.54	16.79	0.00	0.00	0.00	100.00
2A	P2EJA-6	4.81	14.83	19.64	11.32	36.18	32.86	0.01	0.00	100.01
	P2EJA-23	6.02	20.28	26.30	17.33	27.67	28.61	0.00	0.00	99.91
	P2EJA-24	4.56	16.36	20.92	15.71	29.84	33.52	0.00	0.00	99.99
2B	P2EJA-19	6.21	24.50	30.71	34.10	35.03	0.15	0.00	0.00	99.99
	P2EJA-25	9.88	36.50	46.38	24.80	28.70	0.15	0.00	0.00	100.03
Ca	P2EJA-3	20.70	62.70	83.40	9.97	5.87	0.77	0.00	0.00	100.01
	P2EJA-4	8.24	46.87	65.11	14.35	16.37	4.21	0.00	0.00	100.04
	P2EJA-8	9.58	51.70	71.28	12.80	15.87	0.06	0.00	0.00	100.01
	P2EJA-9	30.85	68.75	99.60	0.41	0.00	0.00	0.00	0.00	100.01
	P2EJA-10	26.79	64.02	90.81	7.83	1.34	0.05	0.00	0.00	100.03
	P2EJA-13	21.41	73.96	95.37	4.07	0.56	0.00	0.00	0.00	100.00
	P2EJA-15	25.30	71.20	96.50	3.13	0.38	0.00	0.00	0.00	102.01
	P2EJA-18	25.81	47.35	73.16	12.99	13.81	0.06	0.00	0.00	100.02
	P2EJA-20	23.95	60.89	84.84	13.55	1.63	0.00	0.00	0.00	100.02

DISCUSSION

The relationships between the grain-size volume fractions and the gas permeability (k_G) in Figures 2a and 2b have relatively clearly shown that the role of the mud (<63 μm) fractions and sand (>63 μm) fractions are different in these sedimentary samples. It is suggested that the latter forms the framework of the sedimentary formation from which these samples were obtained, with their intergranular pores contributing to fluid migration, and the mud fractions forming the intergranular pore-filling material that contributes to blocking of the fluid migration. It is generally understood that clay (<2 μm or <4 μm) is the pore-filling material (e.g. Yang and Aplin, 2007), but the results of this study suggest that mud is the pore-filling material for these samples. It is interesting, however, that an increased very fine sand content initially shows a k_G increased effect (Fig. 2a) followed by a decreased effect. This is likely very fine sand performing as framework grains under certain conditions, such as among very fine-grained material, but as pore-filling material under different conditions, such as among larger grains.

Three different trends are seen in the k_G results as a function of mud content relationships (Fig. 5). Two groups of samples show k_G values decreasing with increased mud content, with one

group showing a slightly steeper k_G decrease with increasing mud content than the other. Some of the samples with mud content above 60% show a slight general k_G increase with increased mud content. Samples with the slower k_G decrease with increasing mud content (sample groups 1A, 1B, 1C) have only one differential volume maximum (Fig. 3). Samples with the steeper k_G -mud-content relationship (sample groups 2A and 2B) have two differential volume maximums (Fig. 4). For a formation to have good seal quality, it is necessary that the intergranular pore-filling material, which is the mud content for these sediment samples, must completely fill or exceed these intergranular pore spaces, as shown in Figure 6. The magnitude of the intergranular pore space depends upon the grain packing and grain-size combinations. For an ideal packing of uniform spheres, the intergranular porosities are in the range of 26% to 48% (Mitchell, 1993). The mud content required to fill these intergranular pore spaces is the critical mud content. The concept for clay being the pore-filling material has previously been discussed (Katsube et al., 2006a), using the critical clay content instead of critical mud content. The k_G decreases with increased mud content in Figure 5 because the intergranular pore spaces are filling up with mud and the passages for fluid migration are becoming blocked.

Petrophysical model of mudrock texture

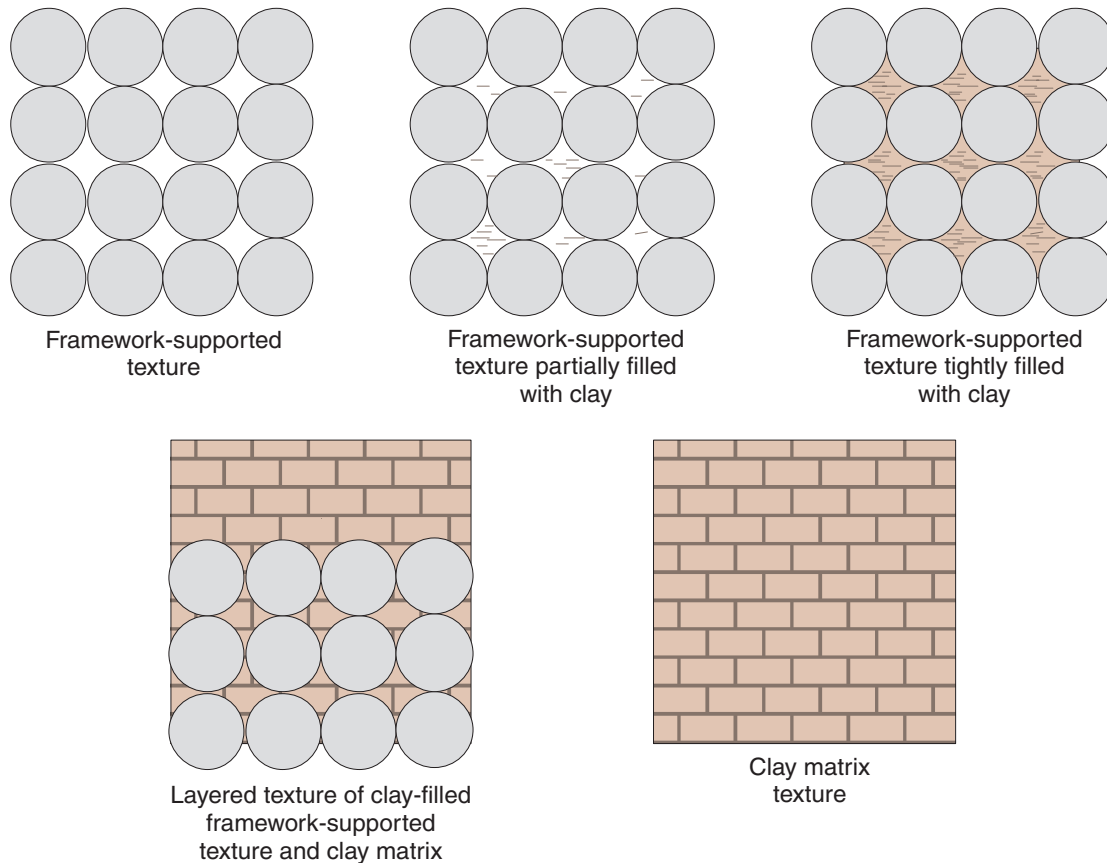


Figure 6. Texture models for framework grain structures with no clay filling (top left), some clay filling (top middle), intergranular pores filled with clay (top right), clay filling exceeding intergranular pore space (bottom left), and the matrix structure with clay only (bottom right)(Katsube et al., 2006b).

When the sediments consist of more than one framework grain-size, and if the smaller framework grains can fit into the intergranular pore spaces of the larger grains, then the intergranular porosity of the larger grains can be reduced below that of the ideal packing of uniform spheres, which is 26–48% (Mitchell, 1993). This would create less space for the mud to fill, or a smaller critical mud content value, implying that the mud would fill the pore spaces of the multi-grain-size framework quicker than the case of the single grain-size framework, and less mud would be required to form a seal. This explains the reason for the k_G –mud-content relationship of the Group 2-DVM samples (Fig. 5), which have two differential volume maximums, to be steeper than that of the samples with the single differential volume maximum (Group 1-DVM). No critical mud content values have been determined in this study; however, the results in Figure 5 suggest that it might be possible to use extensions or modifications of relationships such as those of k_G –mud-content to determine such values.

The slight k_G increase with increased mud content in the ‘Mud’ group (Fig. 5), for the samples with k_G values below 1 mD, is a trend that is unexpected and an explanation for

that relationship is not found in this study. Although mud represents grain sizes of less than 63 μm in this study, it includes various silt grain sizes besides clay (<4 μm), as listed in Table 3. It is possible that these silt grains are not all spherical, but are of various morphologies, some of which might contribute to fluid passages. These could be subjects for future studies.

Although the use of hydraulic permeabilities (k_H) would be reasonable for this type of seal capacity analysis, this study has shown that the use of k_G does provide information of significance on the fluid migration through a sediment. The k_H data in sufficient quantity for these type of samples are difficult to find and are very costly, but should be obtained for future studies of this nature. The few k_G and k_H data that do exist, for identical samples from this area (Katsube et al., 1996, 1999) or for an unconsolidated seafloor sample from the Canadian east coast (Loman et al., 1993; Katsube, 2000), indicate that the k_G values are about 100–5000 times larger than the k_H values. Theoretical equations for permeability (e.g. Brace et al., 1968; Freeze and Cherry, 1979) suggest that under normal conditions, which could imply permeable material, k_H and k_G should be equal.

In extremely low-permeability material, however, the effect of the pore-structure conditions are different from those in permeable material. The k_G usually represents values of a dry material, whereas k_H represents values of a moist material. In such cases, a dry shale for gas flow would have no adsorbed water layers on the pore surfaces to reduce the pore sizes and reduce the k_G value. For a wet shale, however, adsorbed water layers on the pore surfaces would reduce the pore sizes considerably and consequently reduce the k_H value for that liquid migration. Therefore, k_G and k_H values can differ considerably in low-permeability material. In permeable material, the connecting pore sizes can be in the order of 1–100 μm , in which case there would be no or little difference in connecting pore sizes whether they are wet or dry; however, in extremely low-permeability material, such as shale seals, there are many very small connecting pores that are smaller than 3–10 nm (e.g. Katsube, 2000; Bowers and Katsube, 2002). Since the adsorbed water layers on each pore surface could have a thickness in the order of 1 nm or more (Hinch, 1980; Katsube et al., 2000), they could have a significant effect in reducing the effective pore sizes that control fluid migration and result in significantly reduced k_H values.

CONCLUSIONS

Analysis of the relationships between the grain sizes and gas permeability (k_G) of the 28 sedimentary samples, used in this study, show that the grain sizes larger than the fine sand fractions ($>63 \mu\text{m}$) form the framework grains of the sedimentary formation from which these samples were obtained. The same analysis also shows that the mud fraction ($<63 \mu\text{m}$) of these samples, which consists of the clay and silt fractions, is the pore-filling material of the intergranular pores formed by these framework grains.

Two-thirds of these 28 sediment samples have a mud content below 60% with their main content being various grain sizes of sand. Results of using the Wentworth grain-size classification show that the framework grains can be divided into two grain-size distribution groups, one having just one differential volume maximum and the other having two differential volume maximums. While the k_G -mud-content relationships of the two groups both show a k_G decrease with increased mud content, as expected, the group with the two differential volume maximums shows a steeper decrease than the other. This suggests that some of the grains of the smaller differential volume maximum of the group with the two differential volume maximums could be filling the intergranular pore spaces formed by the grains of the larger differential volume maximum and reducing the total intergranular pore spaces of that group. This would allow the mud content to fill these pore spaces faster, and result in the k_G -mud-content relationship to be steeper than the sample group with only one differential volume maximum. This displays an important characteristic of the framework grain-size combinations.

An unexpected k_G -mud-content relationship has been seen for most of the samples that have a mud content exceeding 60%, where a slight increase of k_G with increased mud content is seen. An explanation for this unexpected relationship was not found in this study and its reason is suggested to be investigated in the future. Although the characteristics of hydraulic permeability (k_H) are considered most important in relation to seal capacity, this study has shown that the k_G versus texture characteristics have displayed important characteristics of a seal that may not have been revealed by use of the k_H values.

ACKNOWLEDGMENTS

The authors are grateful to M. Hinton (GSC Ottawa) and B. Medioli (GSC Ottawa) for critically reviewing this paper. The comments and suggestions by both critical reviewers have been very useful for improving the quality of the 'Data analysis' and 'Discussion' sections and of the entire paper. The authors would also like to thank E. Inglis (DDD) for her very constructive and useful comments regarding the text of this paper. Comments by J.B. Percival (GSC Ottawa) have been useful for completing the mineralogical discussions in this paper. The authors are grateful for the advice and support related to this study received from D. Issler (GSC Calgary). The authors would also like to acknowledge the support received from F. Wright (GSC Pacific) for this study.

REFERENCES

- American Petroleum Institute, 1960. Recommended practices for core-analysis procedure; API Recommended Practice 40 (RP 40) American Petroleum Institute, Washington, D.C., p. 55 (first edition).
- Bowers, G.L. and Katsube, T.J., 2002. The role of shale pore-structure on the sensitivity of wireline logs to overpressure; *in* Pressure Regimes in Sedimentary Basins and their Prediction; (ed.) A.R. Huffman and G.L. Bowers; American Association of Petroleum Geologists, Memoir 76, p. 43–60.
- Brace, W.F., Walsh, J.B., and Frangos, W.T., 1968. Permeability of granite under high pressure; *Journal of Geophysical Research*, v. 73, p. 2225–2236.
- Connell-Madore, S. and Katsube, T.J., 2007. Pore-size distribution of samples from the Mallik 5L–38 well, Northwest Territories; Geological Survey of Canada, Current Research 2007–B2, 11 p.
- Dallimore, S.R., Medioli, B.E., Laframboise, R.R., and Giroux, D., 2005. Mallik 2002 Gas Hydrate Production Research Well Program, Mackenzie Delta, Northwest Territories: well data and interactive data viewer; Appendix A *in* Scientific Results from the Mallik 2002 Gas Hydrate Production Research Well Program, Mackenzie Delta, Northwest Territories, Canada, (ed.) S.R. Dallimore and T.S. Collett; Geological Survey of Canada, Bulletin 585.

- Domenico, P.A. and Schwartz, F.W., 1990. *Physical and Chemical Hydrogeology*; John Wiley and Sons, Inc., New York, Chichester, Brisbane, Toronto, Singapore, 790 p.
- Folk, R., 1968. *Petrology of Sedimentary Rocks*; Hemphill's Book Store, Austin, Texas, 170 p.
- Freeze, R.A. and Cherry, J.A., 1979. *Groundwater*; Prentice Hall, New Jersey, 604 p.
- Hinch, H.H., 1980. The nature of shales and the dynamics of hydrocarbon expulsion in the Gulf Coast Tertiary section; *in* Problems of Petroleum Migration, (ed.) W.H. Roberts and R.J. Cordell; American Association of Petroleum Geologists, Studies in Geology, AAPG Publication 10, Tulsa, Oklahoma, 1–18.
- Katsube, T.J., 2000. Shale permeability and pore-structure evolution characteristics; implications for overpressure; *Geological Survey of Canada, Current Research 2000-E15*; 9 p.
- Katsube, T.J., Bloch, J., and Cox, W.C., 1998. The effect of diagenetic alteration on shale pore-structure and its implications for abnormal pressures and geophysical signatures; *in* Proceedings for the Overpressures in Petroleum Exploration Workshop, (ed.) A. Mitchell, R.E. Swarbrick, and J. Dainelli; Elf-EP Memoire-22, April 7–8, 1998, Pau, France, p. 1/9–9/9.
- Katsube, T.J., Dallimore, S.R., Uchida, T., Jenner, K.A., Collett, T.S., and Connell, S., 1999. Petrophysical environment of sediments hosting gas-hydrate, JAPEX/JNOC/GSC Mallik 2L-38 gas hydrate research well; *in* Scientific Results from JAPEX/JNOC/GSC Mallik 2L-38 Gas Hydrate Research Well, Mackenzie Delta, Northwest Territories, Canada, (ed.) S.R. Dallimore, T. Uchida, and T.S. Collett; *Geological Survey of Canada, Bulletin 544*, p. 109–124.
- Katsube, T.J., Dallimore, S.R., Jonnasson, I.R., Connell-Madore, S., Mediolli, B.E., Uchida, T., Wright, J.F., and Scromeda, N., 2005. Petrophysical characteristics of gas-hydrate bearing and gas-hydrate-free formations in the JAPEX/JNOC/GSC et al Mallik 5L-38 gas hydrate production research well; *in* Scientific Results from the Mallik 2002 Gas Hydrate Production Research Well Program, Mackenzie Delta, Northwest Territories, Canada, (ed.) S.R. Dallimore and T.S. Collett; *Geological Survey of Canada, Bulletin 585*, 14 p.
- Katsube, T.J., Grunsky, E., Das, Y., DiLabio, R., McNairn, H., Connell-Madore, S., Gauthier, E., and Scromeda, N., 2006a. Physical model of soil and its implication for landmine detection interference; *in* Proceedings of SPIE (The International Society for Optical Engineering), Detection and Remediation Technologies for Mines and Minelike Targets XI, (ed.) J.T. Broach, R.S. Harmon, and J.H. Holloway; v. 6217, p. 62170N1–N12.
- Katsube, T.J., Issler, D.R., and Connell-Madore, S., 2006b. Storage and connecting pore structure of mudstone-shale and its effect on seal quality: tight shales that may leak; *in* Abstract Volume of AAPG International Conference and Exhibition, November 5–8, 2006, Perth, Australia, p. 60.
- Katsube, T.J., Issler, D.R., and Coyner, K., 1996. Petrophysical characteristics of shales from the Beaufort-MacKenzie Basin, northern Canada; permeability, formation factor, and porosity versus pressure; *in* Current Research 1996-B, Geological Survey of Canada, p. 45–50.
- Katsube, T.J., Scromeda, N., and Connell, S., 2000. Thicknesses of adsorbed water layers on sediments from the JAPEX/JNOC/GSC Mallik 2L-38 gas hydrate research well, Northwest Territories; *Geological Survey of Canada, Current Research 2000-E5*, 6 p.
- Loman, J.M., Katsube, T.J., Correia, J.M., and Williamson, M.A., 1993. Effect of compaction on porosity and formation factor for tight shales from the Scotian Shelf; *in* Current Research, Part E; Geological Survey of Canada, Paper 93-1E, p. 331–335.
- Masch, F.D. and Denny, K.J., 1966. Grain size distribution and its effect on the permeability of unconsolidated sands; *Water Resources Research, Forth Quarter*, no. 4, p. 665–677.
- Medioli, B.E., Wilson, N., Dallimore, S.R., Paré, D., Brennan-Alpert, P., and Oda, H., 2005. Sedimentology of the cored interval, JAPEX/JNOC/GSC et al. Mallik 5L–38 gas hydrate production well, Mackenzie Delta, Northwest Territories; *in* Scientific Results from the Mallik 2002 Gas Hydrate Production Research Well Program, Mackenzie Delta, Northwest Territories, Canada, (ed.) S.R. Dallimore and T.S. Collett; *Geological Survey of Canada, Bulletin 585*, 21 p.
- Mitchell, J.K., 1993. *Fundamentals of Soil Behaviour*; John Wiley & Sons, Inc., New York, Chichester, Brisbane, Singapore, 437 p (second edition).
- Yang, Y. and Aplin, A.C., 2007. Permeability and petrophysical properties of 30 natural mudstones; *Journal of Geophysical Research*, v. 112, 18 p.

Geological Survey of Canada Project Y62